Journal of Anatomy

J. Anat. (2009) **214**, pp607–619 doi: 10.1111/j.1469-7580.2009.01052.x

The anatomy and development of the claws of *Xenopus laevis* (Lissamphibia: Anura) reveal alternate pathways of structural evolution in the integument of tetrapods

Hillary C. Maddin,[1] Leopold Eckhart,[2] Karin Jaeger,[2] Anthony P. Russell[1] and Minoo Ghannadan[2]

[1]*Biological Sciences, University of Calgary, Calgary, Alberta, Canada*
[2]*Department of Dermatology, Medical University of Vienna, Vienna, Austria*

Abstract

Digital end organs composed of hard, modified epidermis, generally referred to as claws, are present in mammals and reptiles as well as in several non-amniote taxa such as clawed salamanders and frogs, including *Xenopus laevis*. So far, only the claws and nails of mammals have been characterized extensively and the question of whether claws were present in the common ancestor of all extant tetrapods is as yet unresolved. To provide a basis for comparisons between amniote and non-amniote claws, we investigated the development, growth and ultrastructure of the epidermal component of the claws of *X. laevis*. Histological examination of developing claws of *X. laevis* shows that claw formation is initiated at the tip of the toe by the appearance of superficial cornified cells that are dark brown. Subsequent accumulation of new, proximally extended claw sheath corneocyte layers increases the length of the claw. Histological studies of adult claws show that proliferation of cornifying claw sheath cells occurs along the entire length of the claw-forming epidermis. Living epidermal cells that are converting into the cornified claw sheath corneocytes undergo a form of programmed cell death that is accompanied by degradation of nuclear DNA. Subsequently, the cytoplasm and the nuclear remnants acquire a brown colour by an as-yet unknown mechanism that is likely homologous to the colouration mechanism that occurs in other hard, cornified structures of amphibians such as nuptial pads and tadpole beaks. Transmission electron microscopy revealed that the cornified claw sheath consists of parallel layers of corneocytes with interdigitations being confined to intra-layer contacts and a cementing substance filling the intercorneocyte spaces. Together with recent reports that showed the main molecular components of amniote claws are absent in *Xenopus*, our data support the hypothesis that claws of amphibians likely represent clade-specific innovations, non-homologous to amniote claws.

Key words amphibian; claw; epidermis; evolution; keratin.

Introduction

The evolution of claws in tetrapods has almost certainly played an important role in the successful exploitation of many aspects of the terrestrial domain. Despite the important consequences of claws, very little is known of their origin and evolution in tetrapods. For the purposes of this contribution, a structure qualifies as a claw if it meets both of the following criteria: (1) it combines both modified integument and skeletal elements in close association with one another, and (2) it is spatially restricted in its occurrence to the distalmost region of the digit. By this nominal definition, claws among extant tetrapods include mammalian claws, hooves and nails, reptilian claws, avian claws (mostly, but not absolutely, confined to digits of the hindlimbs) and the claws of certain frog and salamander species (Fig. 1).

Claws (*sensu lato*, see above) are ubiquitously present in all major amniote clades (with occasional loss in some limbed taxa, e.g. cetaceans). The general anatomy and development of the mammalian claw is well documented (Kato, 1977; Bragulla et al. 2001; Hamrick, 2001, 2003; Homberger et al. 2009, this issue), whereas few studies of reptilian and avian claws have been reported (Alibardi, 2008; Eckhart et al. 2008). The adult mammalian claw consists of a thick, cornified sheath that encases the terminal phalanx of the digit (Fig. 2A). The majority of the cornified claw sheath cells are derived from the proximodorsal surface of the terminal phalanx of the digit by terminal differentiation of the living layers of the epidermis of the germinative matrix (see Homberger et al. 2009, this issue). In the human nail system, the growth of the nail is driven

Correspondence
Hillary C. Maddin, Biological Sciences, University of Calgary, 2500 University Drive NW, Calgary, Alberta, Canada, T2N 2N4.
E: hcmaddin@ucalgary.ca

Accepted for publication *11 January 2009*

by cell proliferation in the nail germinative matrix, whereas the distal region of the epidermis does not contribute to the nail (Jaeger et al. 2007). A similar growth pattern may also be present in the model reptile *Anolis carolinensis* (Eckhart et al. 2008), whereas the formation of the claw may occur more distally in other reptiles (Alibardi, 2008). The conversion of the living cells of the human nail epidermis into the inert corneocytes of the cornified nail represents a form of programmed cell death, which is accompanied by degradation of the nuclear DNA (Jaeger et al. 2007).

Lissamphibian claws

Given the substantial contribution of cornified tissue to the formation of amniote claws (Kato, 1977; Bragulla et al. 2001; Hamrick, 2001, 2003; Homberger et al. 2009, this issue), it is unsurprising that claws or claw-like structures are largely absent from lissamphibians, as they exhibit a minimally cornified epidermis. Despite this, hard, cornified integumentary structures resembling amniote claws in general appearance are present in some lissamphibian species (Figs 1 and 2B; Noble, 1931; Duellman & Trueb, 1994). The hynobiid salamanders *Onychodactylus japonicus* and *Onychodactylus fischeri* have claws on both fore- and hindlimbs. The sirenid salamander *Pseudobranchus striatus* lacks hindlimbs but has claws on all four digits of the forelimbs.

Among anurans, pipids are the only group known to possess claws. In the two genera with claws, *Xenopus* and *Hymenochirus*, the claws appear as black cone-shaped caps on the tips of the first three pedal digits. The general anatomy of these structures in *Xenopus laevis* was recently described and hypotheses relating to their growth presented

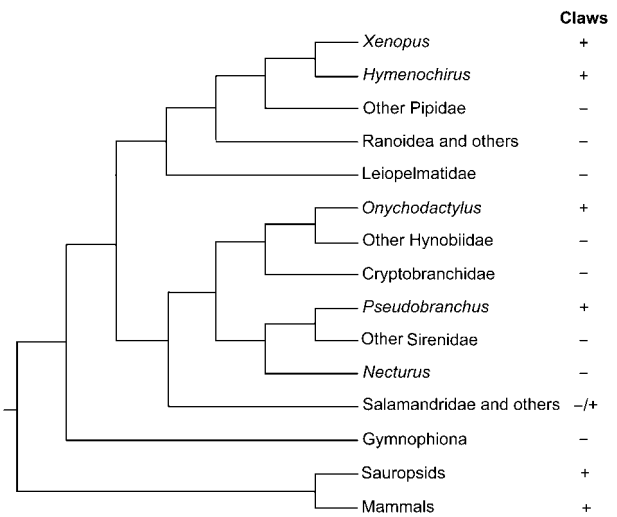

Fig. 1 Distribution of claws among tetrapod taxa. The presence (+) or absence (–) of claws is mapped onto a phylogenetic tree that is based on San Mauro et al. (2005), with relationships among Sirenoidea being shown according to Frost et al. (2006).

(Maddin et al. 2007). Based on differences in both the anatomy and the inferred pattern of growth, Maddin et al. (2007) suggested that the claws of *X. laevis* evolved independently of those of amniotes. We herein seek to improve the current understanding of claw origin and evolution by examining the anatomy and development of claws in a lissamphibian, and by comparing them with those of amniotes. We employ new methods to examine previous hypotheses by exploring the pattern of claw structure and growth.

Data accumulated from ultrastructural investigations, via transmission electron microscopy (TEM), on the anatomy of the epidermal component of the claws of *X. laevis* are presented here, along with observations on the development of the cornified claw sheath from its first appearance in late tadpole stages through to metamorphosis. The latter approach involved both gross morphological and microstructural observations. In addition, we investigate the pattern of cell proliferation and cornification-associated cell death using *in situ* labelling assays. These data are first discussed in the context of what is known about similar structures of mammalian amniotes, which are then appraised in the context of their implications for the evolution of claws among tetrapods.

Materials and methods

Animal housing and care

Freshly sacrificed adult specimens of *X. laevis* were acquired from breeding and early development research programs already in progress at the University of Calgary, where they were housed and euthanized according to University of Calgary Animal Care protocols. Embryos (NF 47) were also obtained from these programs and were raised in 10-gallon aquaria filled with aerated, dechlorinated tap water kept at room temperature.

Tissue collection

Adult tissue

Fore- and hindlimb digits (clawed and non-clawed) and skin from the back region were dissected from freshly sacrificed adult male *X. laevis* and immediately fixed in 10% neutral-buffered (PBS) formalin for 24 h and rinsed in running tap water for another 24 h. Samples were then dehydrated through a series of ethanol solutions (1 h in 30%, 50%, 70% and 70% each) and stored in fresh 70% ethanol prior to histological and immunohistochemical preparations.

Froglet tissue

Pedal digits (clawed and non-clawed) and skin from the back region was dissected from freshly euthanized froglets (NF 66, recently transformed) and was immediately fixed in glutaraldehyde for TEM observation (details below).

Developmental series

A developmental series of *X. laevis* was assembled by raising recently hatched embryos. At the onset of hindlimb development,

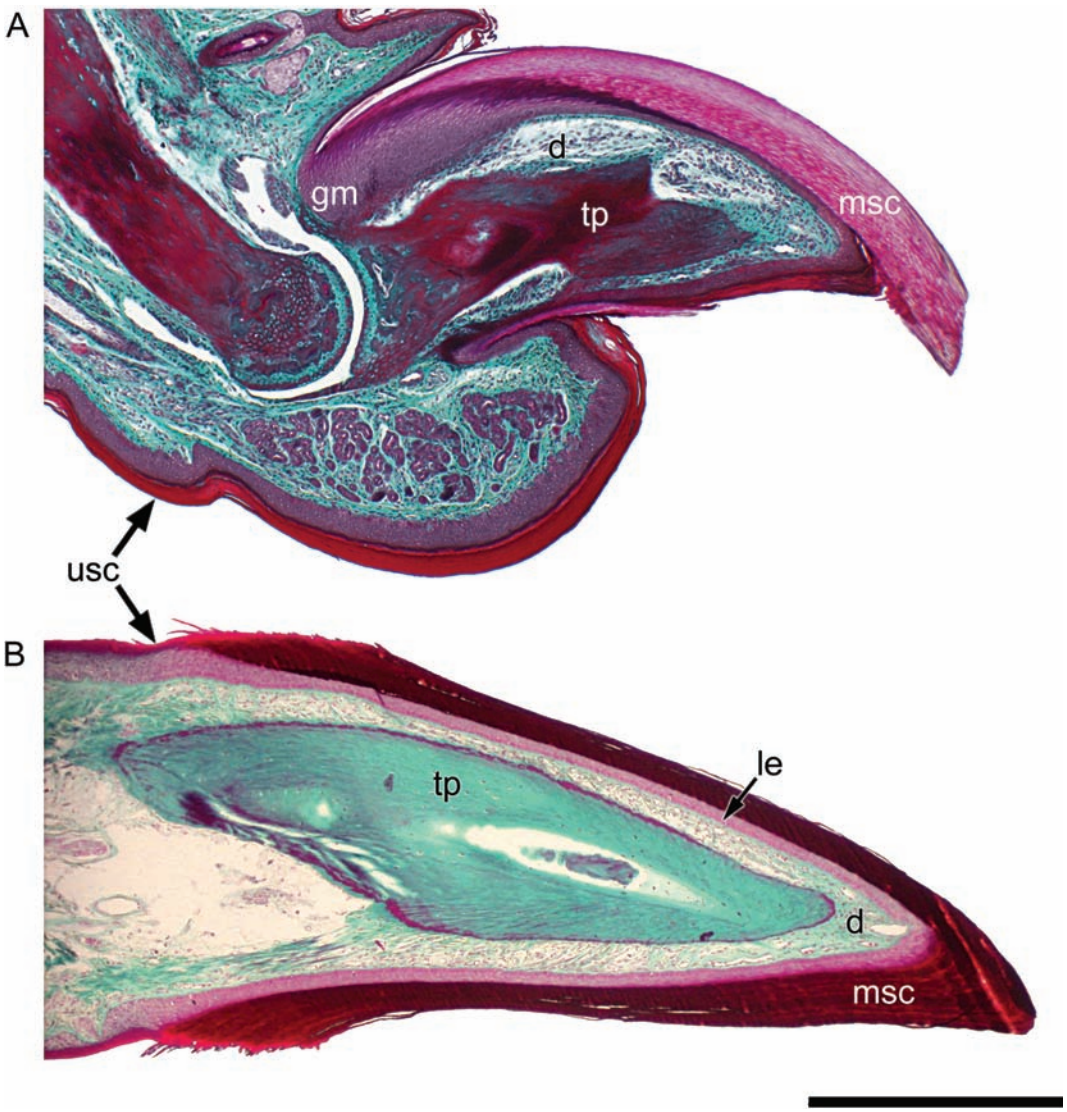

Fig. 2 Comparison of the claws of *Xenopus* and *Mus*. (A) Longitudinal section of an adult mouse claw, and (B) longitudinal section of the claw of *Xenopus laevis* (used with permission from Maddin et al. 2007). The cornified layers of the epidermis form the claw sheaths in the mouse and in *Xenopus*. Scale bar 1 mm. Abbreviations for all figures: bg, basal germinative layer; d, dermis; ds, desmosome; g, gland; gm, germinative matrix region; is, intermediate spinous layers; le, living epidermal layers; lm, lateral margin; rl, replacement layer; mp, melanophore; msc, modified corneocytes of the corneous layer; tp, bony terminal phalanx; tp*, cartilaginous terminal phalanx; usc, unmodified corneocytes of the corneous layer.

animals were regularly inspected microscopically for evidence of claw sheath appearance and individuals bearing claws were staged according to the normal table of Nieuwkoop & Faber (1967). The earliest developmental stage visibly bearing claws is NF 59. Thus, tadpoles at stage NF 58 were also collected to observe the state of epidermal organization immediately prior to claw sheath appearance. Developmental stages NF 58 (pre-metamorphic tadpole) through to NF 66 (post-metamorphic froglet) are represented in the developmental series. Animals were euthanized and tissue samples were immediately fixed in 10% neutral-buffered formalin for 24 h, rinsed in running tap water for 24 h and then dehydrated to 70% ethanol through a series of ethanol solutions (1 h in 30%, 50%, 70% and 70% each) and stored in 70% ethanol prior to histological preparation.

Histological preparations

Xenopus laevis material

Tissue samples were rehydrated through a series of ethanol solutions and water for 1 h in 50% and 30% each twice in distilled water and immersed in Cal-ex® (Fisher Scientific) overnight to demineralize the bone. The tissue samples were then rinsed in running tap water for 2 h, dehydrated through a series of ethanol solutions for 1 h in 30%, 50%, 70%, 80%, 95%, 100% and 100% each, and immersed in CitriSolve solvent (Fisher Scientific) solution for 30 min to facilitate paraffin wax infiltration. This step was repeated in fresh solution for another 30 min. Infiltration with paraffin wax occurred in a sealed vacuum oven overnight.

Tissue blocks of the limbs and back skin from the developmental series were sectioned at 5 μm, mounted on slides coated in 3-aminopropyltriethoxysilane adhesive, and stained with haematoxylin (Gill's variant) and eosin to optimally visualize the immature tissue. Material from the adult specimen was sectioned at 7 μm, and stained with both haematoxylin and eosin and Masson's trichrome following the protocol of Witten & Hall (2003), with Mayer's acid haematoxylin replacing Gill's modified haematoxylin, to optimally visualize the fully differentiated tissue.

Mouse material

A tissue block containing a 10% neutral-buffered (PBS) formalin-fixed, paraffin-embedded hindlimb from a 3-month-old female C57BL/6J mouse was longitudinally sectioned at 5 μm and examined for comparative purposes. Slides were stained using Masson's trichrome (Goldner's modification).

Transmission electron microscopy

Fresh tissue samples excised from a recently sacrificed froglet was immediately fixed in 2.5% glutaraldehyde in 0.1 M sodium cacodylate buffer at pH 7.2–7.4 for 72 h. The tissue samples were rinsed three times, for 10 min each, in 0.1 M sodium cacodylate buffer and post-fixed for 1 h in 1% osmium tetroxide in 0.1 M cacodylate buffer. The tissue samples were again rinsed three times, for 10 min each, in doubly distilled water and dehydrated through a series of acetone solutions for 10 min in each step (30%, 70% and 95%, 3× in 100%). Embedding was performed by transferring the tissue samples through a series of acetone : resin (Spurr's resin) mixtures (3 : 1, 1 : 1, 1 : 3) for 1 h each, and then immersing them in 100% resin three times, for 1 h each. The tissue samples were placed into embedding molds with fresh resin, and polymerized at 60 °C overnight.

The resin blocks were sectioned at 70 nm, the slices mounted on grids, and stained for 15 min in 2% uranyl acetate and then 7 min in Reynold's Lead Citrate before imaging. Observation was achieved using a Hitachi H7000 Transmission Electron Microscope (Microscopy Imaging Facility, University of Calgary).

Immunohistochemistry and transferase-mediated fluorescein-dUTP nick end labelling (TUNEL) assay

Formalin-fixed (10% neutral-buffered formalin), 70% ethanol-preserved hindlimbs and forelimbs from adult male *X. laevis* (University of Calgary) were embedded in paraffin and sectioned at 4 μm. To avoid damage to the antigen epitopes, demineralization was not performed on samples used for immunohistochemistry and TUNEL analysis. Immunohistochemistry was conducted as previously described (Fischer et al. 2007). Briefly, heat antigen retrieval involving two 5-min bouts of microwave treatment at 500 W in target retrieval solution (DakoCytomation, Glostrup, Denmark) was performed on the sections. Endogenous peroxidase was blocked by incubation in 0.3% H_2O_2/methanol. To block non-specific labelling, the sections were pre-incubated in sheep serum (1 : 10) in 2% BSA-PBS, pH 7.2 for 30 min at room temperature, and subsequently incubated at 4 °C overnight with a monoclonal mouse antibody against proliferating cell nuclear antigen (PCNA), clone PC10 (Calbiochem, Nottingham, UK, dilution 1 : 40). Incubation with the corresponding isotype at the same dilution served as negative control. After washing, slides were incubated with biotinylated sheep anti-mouse immunoglobulin (Amersham Biosciences, Chalfont, UK, dilution 1 : 200) and exposed to HRP-streptavidin–biotin complex (DakoCytomation). 3-Amino-9-ethylcarbazole was used as chromogen (DakoCytomation). The TUNEL assay was performed with the *in situ* cell death detection kit (Roche Diagnostics, Mannheim, Germany) according to the manufacturer's instructions. Negative control reactions were carried out by omitting terminal deoxynucleotidyl transferase. Hoechst 33258 (Sigma-Aldrich, Vienna, Austria) was used as a nuclear counterstain.

Results

General anatomy of the claw of adult *Xenopus laevis*

In adults, the claws of *X. laevis* are black, roughly cone-shaped structures that are located at the tips of the first three pedal digits in both males and females. In longitudinal section the cornified claw sheath is triangular in shape with a slight ventral curvature at the distal tip. In cross-section the cornified claw sheath is ovoid in outline, being slightly compressed dorsoventrally (Fig. 3). On the ventral surface

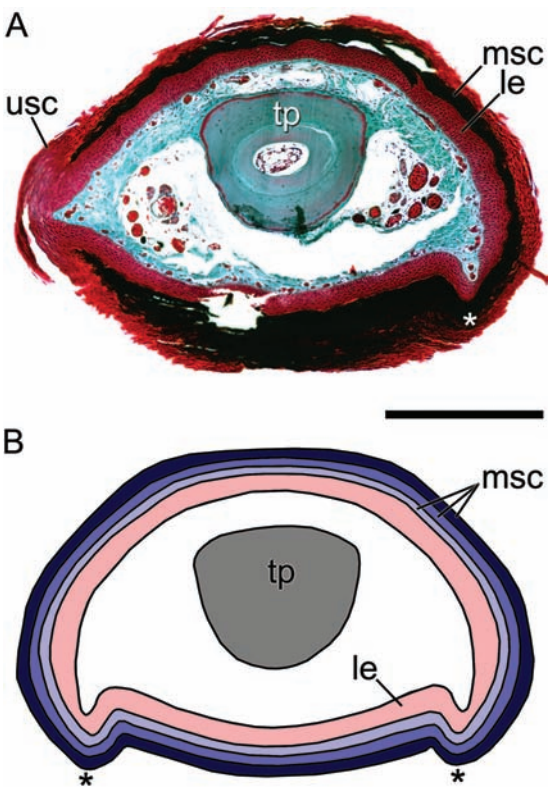

Fig. 3 Cross-sectional view of the claw of *Xenopus laevis*. (A) Histological image of a slightly oblique cross-section showing the roughly ovoid shape of the cornified claw sheath. This section is near the proximal base of the cornified claw sheath, therefore remnants of the older unmodified corneocyte layers are present atop of the younger modified corneocyte layers of the claw sheath. (B) Schematic reconstruction of an ideal cross-section of the claw of *X. laevis*. The three corneocyte layers depicted (light, medium and dark blue) wrap around the lateral and medial surfaces of the digit tip as continuous layers. A pair of ventral ridges (asterisks) formed by the epidermis of the cornified claw sheath extend proximodistally along the length of the claw. Scale bar 1 mm.

the lateral and medial margins of the cornified claw sheath are pinched to form proximodistally oriented ridges (asterisks; Fig. 3) that extend the entire length of claw. The thick epidermal component of the claws in *X. laevis* closely envelops the terminal phalanx of the digit (Figs 2B and 3), like that of the mouse claw (Fig. 2A). The organization of the claw epidermis is consistent with that of typical amphibian stratified epidermis in that the four regions [basal germinative layer, intermediate spinous region, replacement layer, and cornified layer (Budtz & Larsen, 1973)] are present and clearly recognizable throughout the entire claw region. The microstructure of the basal germinative layer, intermediate spinous layers, and replacement layer (Fig. 4C) histologically resemble their unmodified non-claw region counterparts.

The cornified claw sheath epidermis, however, is modified, differing substantially in several respects from that of unmodified epidermis of non-clawed digits and that of the back region. The cornified claw sheath is composed of multiple layers of corneocytes (Fig. 4C), in contrast to the single layer of corneocytes present in unmodified epidermis. The corneocyte layers in the cornified claw sheath are arranged in a parallel fashion and wrap around the lateral and medial surfaces as well as the tip of the digit as continuous layers (Figs 2B and 3). The basalmost layers extend the furthest proximally and successively more superficial corneocyte layers terminate slightly more distally to the layer immediately below.

The corneocytes forming the claw sheath are dark brown and, as a result, their internal cellular structure is obscured at the light microscopy level. This differs from the condition seen in the corneocytes of unmodified epidermis, in which the cytoplasm is less dense, and nuclear remnants and mucous granules are still visible. The modified claw corneocytes, however, resemble other keratinizing structures, such as the nuptial structures (Fig. 4A) and mouthparts of larvae in these respects. There is an abrupt transition between the epidermis of the cornified claw sheath and the unmodified epidermis. The layers superficial to the basal germinative layer in the unmodified epidermis are not continuous with their corresponding layers in the modified cornifying epidermis of the claw (Fig. 4B). The basalmost layers of the corneocytes in the cornified claw sheath contact cells of the intermediate spinous region of the adjacent unmodified epidermis, whereas the most superficial corneocyte layers are not continuous with any cell layers, except for fragments of unmodified epidermis that became detached from the surface of the digit during claw sheath growth (usc; Fig. 4B).

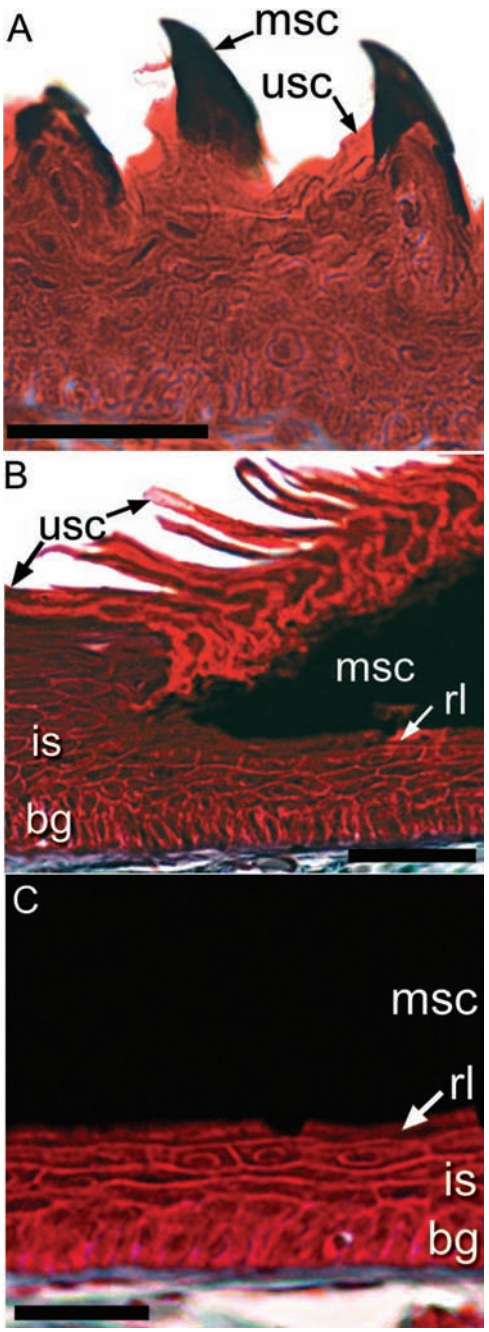

Fig. 4 Close-up views of epidermis from forelimb and hindlimb digits showing details of the modified epidermis forming hard keratinous structures in *X. laevis*. (A) Epidermis from the ventral surface of a forelimb digit showing the dark hook-like nuptial structures comprising modified corneocytes (msc) with a similar distinctive, dark appearance to those of the cornified claw sheath in comparison with the adjacent unmodified corneocytes (usc). (B) Close-up view of a section through the epidermis of the dorsal surface at the base of the claw of *X. laevis* showing the abrupt change at the border between the modified claw sheath corneocytes and the adjacent unmodified corneocytes. (C) Close-up view of the claw region epidermis of *X. laevis* midway along the length of the claw, revealing the four epidermal layers typical of unmodified epidermis and the dramatically modified cornified layer. Masson's trichrome. Scale bars 50 μm.

Development of the claw of *Xenopus laevis*

The first visible sign of the formation of all three cornified claw sheaths occurs in tadpoles at stage NF 59 (Figs 5B and 6B). Although tadpoles at the NF 58 stage do not show any

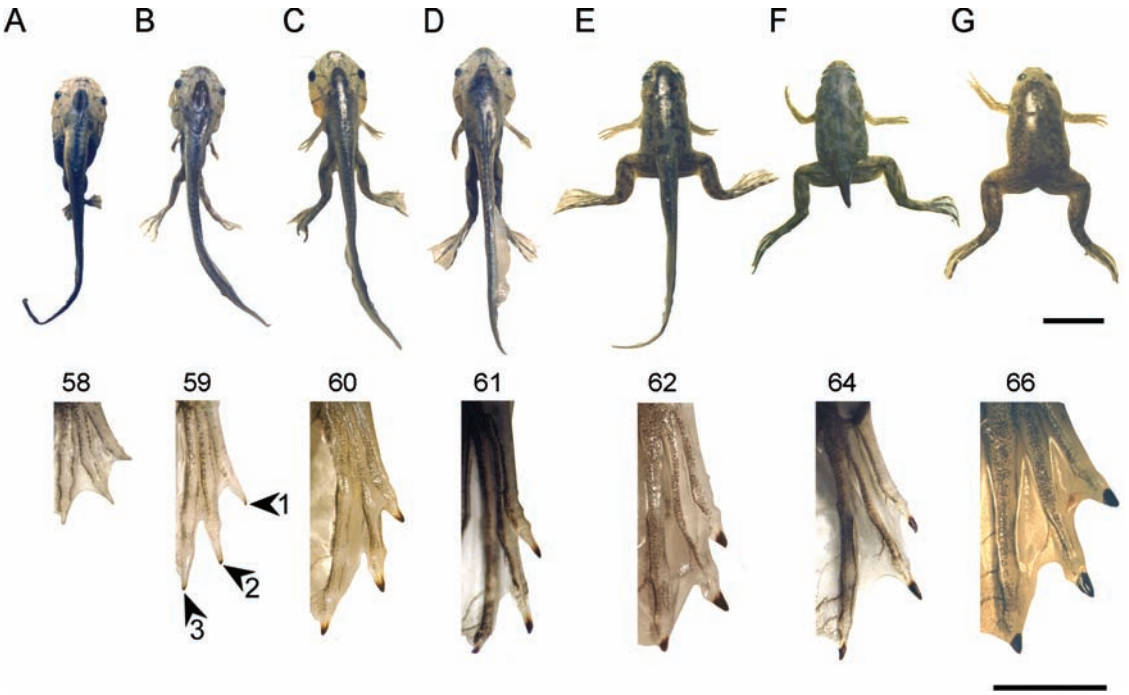

Fig. 5 Developmental series of *X. laevis* from NF 58 stage (no claws present) to NF 66 stage (recently transformed froglet) shows the first appearance of cornified claw sheath and their subsequent growth. Upper row (A–G): preserved whole specimens of the stages documenting claw development. Scale bar 1 cm. Lower row: right pes in dorsal view of the stages illustrated in the upper row. Scale bar 3 mm.

visible signs of a cornified claw sheath, light microscopy reveals that the epidermis at the tips of the future claw-bearing digits has already locally reorganized into a stratified epithelium (Fig. 6A, inset), whereas the unmodified epidermis over the rest of the body exhibits the typical larval bilayered condition. The epidermis is also stratified at the tips of pedal digits four and five at stage NF 59 (data not shown), although these digits do not form claw sheaths.

At stage NF 59, the claw rudiments appear as dark dots at the tips of the claw-bearing digits (Fig. 5B). Light microscopy reveals a small region containing a single layer of modified light to dark brown corneocytes at the tip of the digit (Fig. 6B). Deep to the cornified layer the epidermis is stratified and resembles that of normal post-metamorphic epidermis (Budtz & Larsen, 1973). The degree of stratification of the epidermis decreases proximally, and from about the level of the articulation of the terminal and penultimate phalanx, the epidermis is bilayered, as is typical for the larval condition of unmodified epidermis.

As claw development progresses through stages NF 59–64 the blackened tip increases in both thickness and extent (Fig. 5C–F). The thickening of the cornified claw sheath results from the retention of the older sheath corneocytes while new generations are added basally (Fig. 6C–E). The lengthening of the cornified sheath, as revealed by light microscopy, is due to the appearance of modified corneocytes that extend more proximal than do the older, more superficial layers (Fig. 7). The stratification of the epidermis remains confined to the digital tip, although it extends farther proximally through stages NF 59–64. The remainder of the digit remains covered by the larval-type unmodified epidermis. The claw continues to grow in this pattern through metamorphosis (stages NF 64–66). At stage NF 66 (Fig. 5G), which corresponds to that of a recently transformed froglet, the cornified claw sheath consists of 10–12 corneocyte layers. The sheath develops a slight ventral curvature at the tip, possibly due to differential rates of proliferation between dorsal and ventral surfaces, and this shape is maintained in the adult to varying degrees.

Epidermal proliferation and death in the claws of *Xenopus laevis*

Insight into cell proliferation and cell death in modified epidermis forming the cornified claw sheath, in comparison with that of the adjacent unmodified epidermis, was obtained using immunohistochemical analysis with an antibody against the proliferating cell nuclear antigen (PCNA). In the basalmost layers of the modified claw epidermis many nuclei stained strongly, indicating a high rate of cell proliferation (Fig. 8A). Unlike cell proliferation in the mammalian claw, which is largely restricted to the proximally located germinative matrix and only rarely detectable in the more distal epidermis of the nail or claw bed (de Berker & Angus, 1996; Plikus et al. 2004; Jaeger et al. 2007), cells producing the cornified claw sheath in

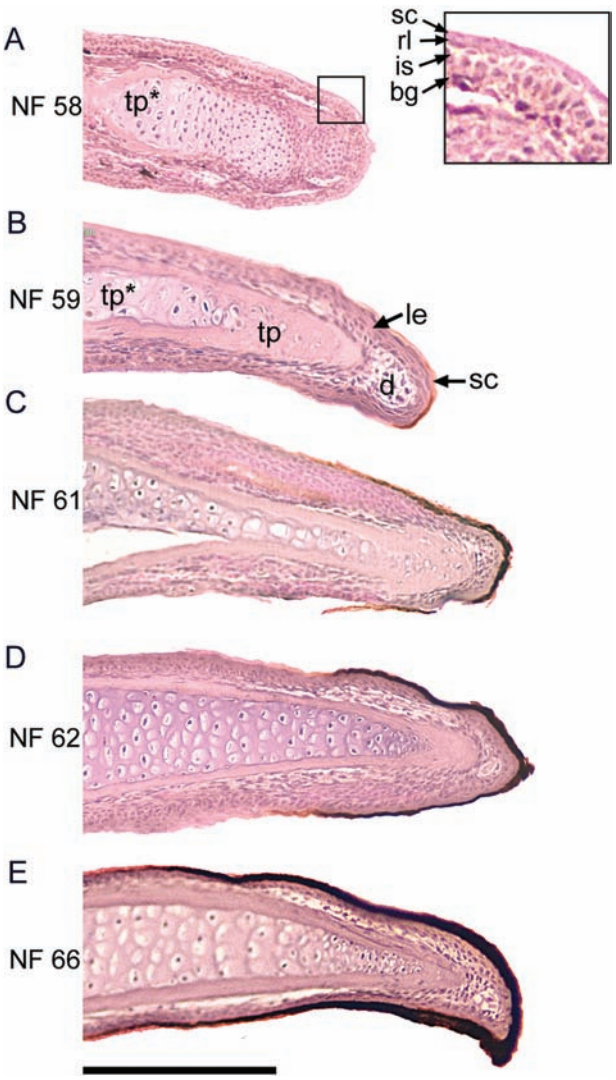

Fig. 6 Longitudinal sections of the left pedal digit I showing the pattern of claw sheath growth in *X. laevis*. (A) There is no sign of a claw in NF stage 58 but the epidermis is locally stratified (inset of digit tip). (B) Modified claw sheath corneocytes appear at NF stage 59. (C–E) Sheath growth proceeds in the proximal direction by the addition of more proximally extending modified claw sheath corneocyte layers basal to the older layer and sheath thickness increases as corneocytes are retained. Haematoxylin and eosin. Scale bar 200 μm. Abbreviations in Fig. 2.

X. laevis proliferate uniformly along the entire length of the claw, both dorsally (Fig. 8A) and ventrally (data not shown). PCNA-positive nuclei were also abundant in the adjacent unmodified epidermis (Fig. 8B).

TUNEL analysis, which specifically reveals DNA fragments with free 3′-OH ends, determined the pattern and mode of cell death in the epidermis of the claw of *X. laevis*. Such DNA fragments have been described in *X. laevis* cells undergoing apoptosis (Estabel et al. 2003) and in cornifying cells of the human epidermis and nail germinative matrix (Jaeger et al. 2007). TUNEL-positive nuclei were detected in the replacement layer in the claw sheath of *X. laevis* (Fig. 9A) but not in the adjacent unmodified epidermis from the same animal (not shown in figures). Notably, few cells of the replacement layer underneath the cornified claw sheath contained nuclei, all of which were labelled. This indicates that the particular specimen shown in Fig. 9A was fixed in the late phase of the conversion of living epidermal cells of the replacement layer into inert corneocytes of the cornified claw sheath. In a different specimen the opposite was observed, in that the replacement layer of the unmodified adjacent epidermis contained TUNEL-positive nuclei (Fig. 9B), whereas the modified claw region epidermis did not. This reveals that the conversion of living epidermal cells into corneocytes is not synchronous between the cornified claw sheath region and the unmodified regions of the digit. Also, the layer containing TUNEL-positive nuclei was only faintly brown, whereas the more superficial layers of the cornified claw sheath were dark brown. It is therefore likely that DNA breakdown in the replacement layer precedes the synthesis of the dark colour during cornification.

Ultrastructure of the claw of *Xenopus laevis*

The modified epidermis of the claws of fully transformed froglets, the unmodified epidermis of digits with no claws, and epidermis of the back region were compared using transmission electron microscopy. The epidermis of the back and the unmodified digits exhibited the typical condition previously described for anuran epidermis, including the three living layers and a single cornified layer (Budtz

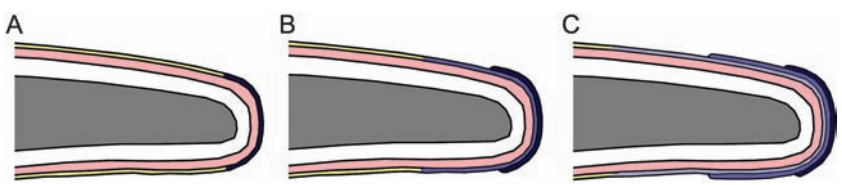

Fig. 7 Schematic illustration of the pattern of claw sheath development in *X. laevis*. (A–C) Successively older stages in the sheath development sequence. Initial differentiation of modified sheath-type corneocytes occurs at the distal tip of the digit (A, dark blue). Subsequent differentiation takes place underneath this layer and extends further proximally (B, medium blue), with successive additions extending even further proximally (C, light blue). Grey, terminal phalanx; pink, living epidermal layers; yellow, unmodified corneocytes of adjacent epidermis.

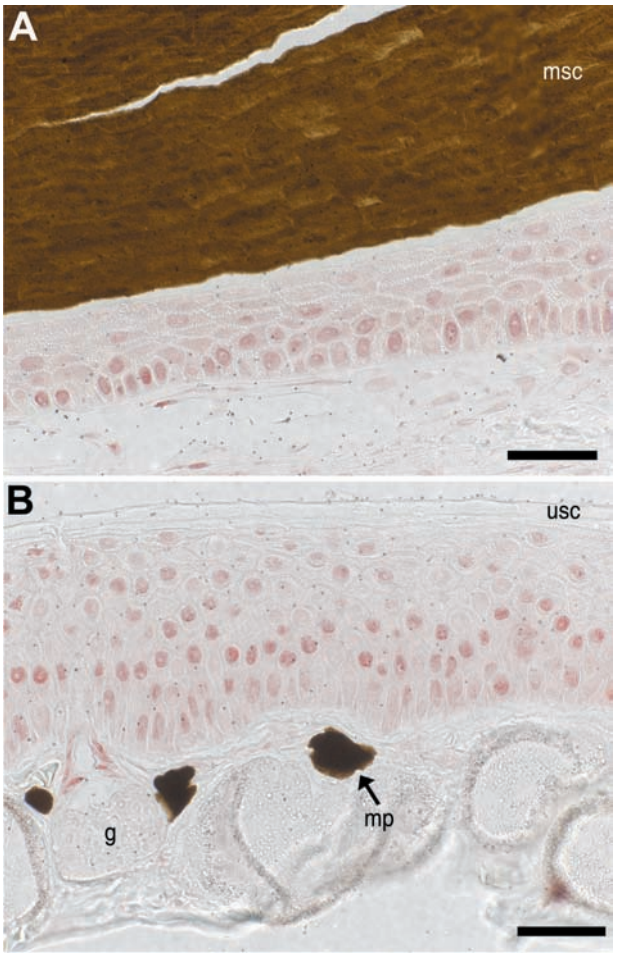

Fig. 8 Immunostaining of proliferating cell nuclear antigen (PCNA) of the modified claw epidermis of *X. laevis* shows the proliferation of epidermal cells contributing to the cornified claw sheath is uniformly distributed underneath the entire length of the claw (A), a pattern like that observed in the unmodified epidermis of the digit (B). PCNA-positive nuclei are stained red. Note that haematoxylin counterstaining has been omitted. Scale bar 40 μm.

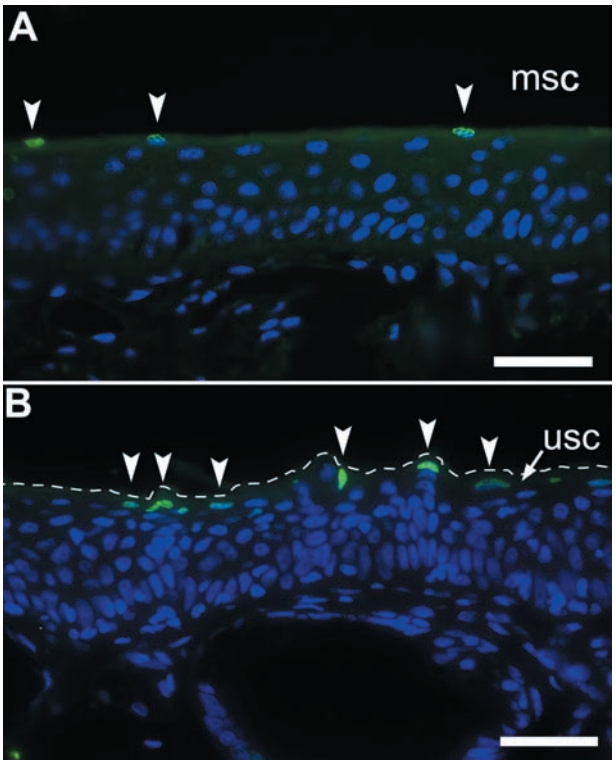

Fig. 9 Detection of DNA fragmentation in the epidermis of *X. laevis*. Thin-sections of digits were subjected to transferase-mediated fluorescein-dUTP nick end labelling (TUNEL) to visualize DNA fragments. (A) TUNEL-positive DNA fragments (green nuclei, arrowheads) were seen in the replacement layer underneath the modified claw sheath epidermis, (B) as well as in replacement layer of the unmodified epidermis, sampled from a different animal. Absence of concomitant TUNEL-positivity in modified claw and unmodified epidermis of the same sample (not shown) may indicate that DNA breakdown occurs in a non-simultaneous manner at both sites. The thick corneous layer of the claw sheath occupies the entire black space at the top of panel (A). In (B), the superficial border of the epidermis is marked by a discontinuous line. Scale bar 40 μm.

& Larsen, 1975; Alibardi, 2001). The cornified layer, however, was not clearly discernible in some regions of the clawless digits. The epidermis forming the cornified claw sheath, in contrast, exhibited several differences from that of the unmodified epidermis.

Most strikingly, claw corneocytes are nearly opaque, resulting in a well-defined boundary between the replacement layer and the claw sheath corneocytes (Fig. 10A). However, intracellular structures of the corneocytes, probably corresponding to remnants of organelles, were seen occasionally. Remarkably, there appear to be fewer large mucous granules in the living layers underneath the cornified claw sheath (Fig. 10A) in comparison with the epidermis at the tip of the clawless digits (Fig. 10B). Within the cornified layers of the claw sheath, the resolution of the intracellular structures is obscured by the dark colouration of the cells (Fig. 10C). The borders of the corneocytes, however, are clearly visible, and their lateral margins are highly interdigitated, resembling the condition seen in the replacement layer underneath the cornified sheath corneocytes (Fig. 10D) and the cornified layer of unmodified epidermis (Fig. 10E). The contours of these interdigitations bear large desmosomes. Sporadic patches of interdigitations also occur on the apical and basal surfaces of the sheath corneocytes, but it is unclear whether these, too, bear desmosomes. Large, expansive desmosomes are also found on the smooth apical surface of the replacement layer cells lying underneath the sheath corneocytes (Fig. 10F). These appear, in general, to be wider, and to be more closely packed than those at the equivalent interface in the unmodified epidermis. The narrow extracellular spaces are filled with a grainy matrix of uncertain biochemical identity.

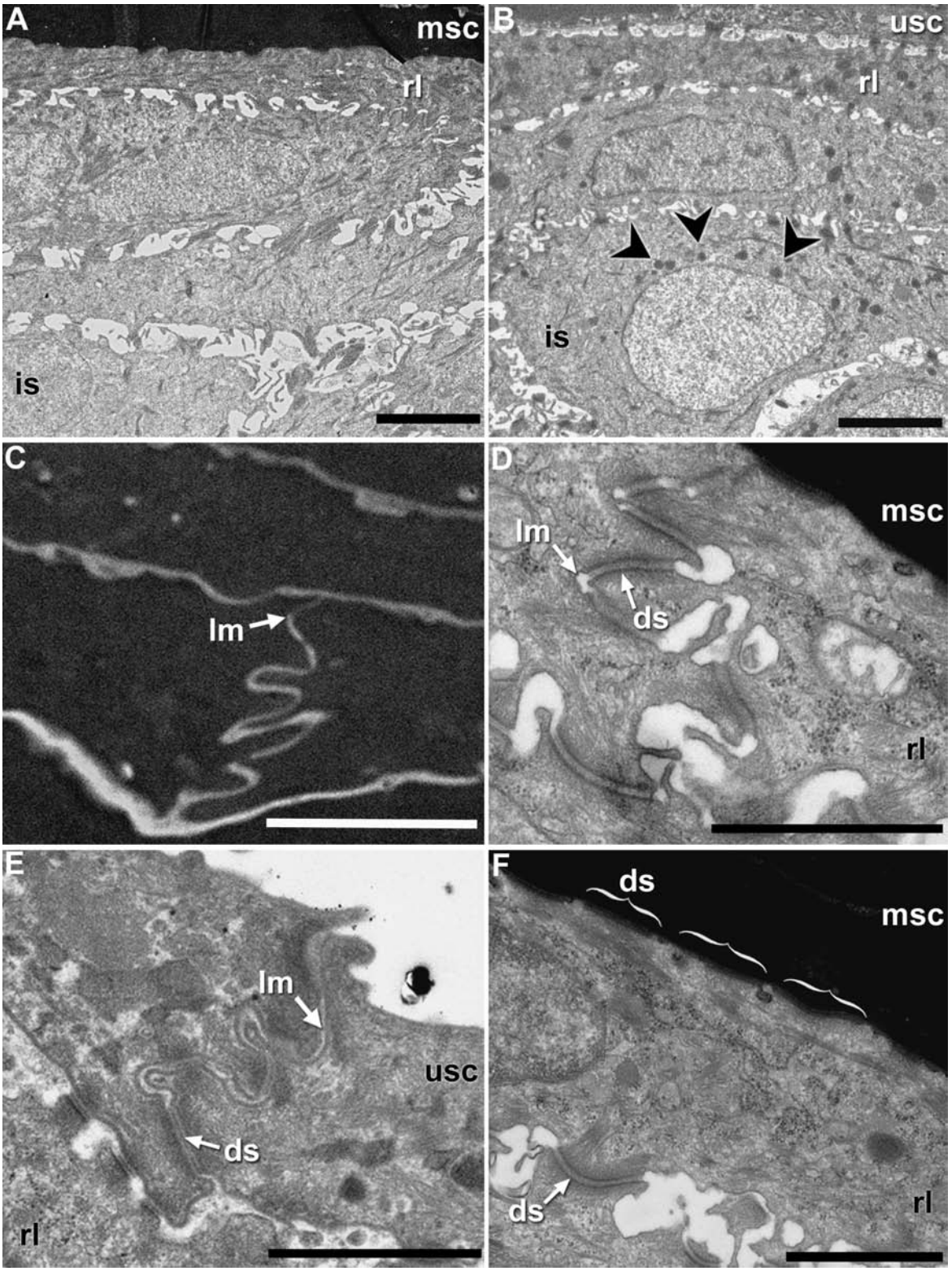

Fig. 10 TEM micrographs of the modified claw and unmodified epidermis of *X. laevis*. Longitudinal section through the claw (A) and the tip of a non-clawed digit (B) comparing the overall epidermal organization. Large mucous granules (arrowheads) are more prevalent in unmodified epidermis than in the modified claw region epidermis (scale bars 5 μm). (C) Close-up of the modified claw sheath corneocytes. Highly interdigitated cell borders are restricted to the lateral borders of the corneocytes of the cornified claw sheath and resemble those seen in the replacement layer under claw (D), and the corneous layer of unmodified digit epidermis (E). (F) The replacement layer and claw are held in close contact by numerous, elongate desmosomes. Scale bars 1 μm. Abbreviations in Fig. 2.

Discussion

Our observations of the anatomy and development of the epidermal component of the claws of *X. laevis* complement those of previous studies (Maddin et al. 2007) and provide new insights into the nature of the keratinization process that leads to the formation of claws in this non-amniote species. This, in turn, provides valuable information for assessing patterns of evolution of claws in tetrapods. Whereas there is little doubt that both the non-amniote and amniote claws rely on a process of keratinization that is homologous for all tetrapods (Alibardi & Toni, 2004), the anatomy and development of the epidermal component of the claws of *X. laevis* differ sufficiently from those of mammalian amniotes to suggest an independent evolutionary origin of these epidermal modifications in these two tetrapod groups.

Comparison of cornified claw epidermis with unmodified epidermis in amphibians

Several important features characterize epidermal differentiation in the unmodified epidermis of lissamphibians. These include the accumulation of mucous granules in apical epidermal cells, the degradation of cytoplasmic organelles, and the eventual disruption of desmosomal junctions between cell layers to permit shedding of the old cornified layer during moulting (Parakkal & Matoltsy, 1964; Budtz & Larsen, 1973; Fox, 1986; Alibardi, 2001). The epidermis of the clawless digit tips in *X. laevis* exhibits these features and conforms closely to the condition typical anuran epidermis. The modified epidermis of the claw region, however, differs from that of unmodified epidermis in several interesting respects, which are discussed below.

In the epidermis of clawless digits, large mucous granules accumulate in close association with the nucleus within the cytoplasm of the cells of the spinous layer (Lavker, 1974; Budtz & Larsen, 1975). These large granules have been hypothesized to have an interkeratin matrix role, similar to the keratohyalin granules of mammals (Alibardi, 2003). An increased number of large mucous granules relative to that of other anurans, such as *Rana,* has also been described for the more terrestrial bufonid anurans (Jorgensen & Larsen, 1964; Bani, 1966), indicating a positive correlation between the number of mucous granules and the degree of cornification (Maddin et al. 2007). The observations presented here seem to contradict this correlation, as large mucous granules were observed only sporadically in the spinous and replacement layers underneath the heavily cornified claw sheath. It is possible that this scarcity of mucous granules is due to the time at which the epidermis was collected (i.e. early stage of differentiation; Budtz & Larsen, 1975); however, this condition was observed in all individuals examined.

Another major difference observed between the modified epidermis of the claw and unmodified epidermis is the colour of the corneocytes forming the cornified claw sheath. Corneocytes of the epidermis are generally transparent in unstained sections. By contrast, the corneocytes of the claw sheath in *X. laevis* are dark. In histological preparations they are virtually opaque. The dark brown colour is uniform and obscures nearly all internal detail of the corneocytes at the microstructural level. The colour is not derived from melanosomes, because neither light microscopy (Fig. 8) nor electron microscopy (Fig. 10) revealed such organelles in cells of the modified epidermis forming the claw sheath. The intense colouration is resistant to treatment with hydrogen peroxide (H. Maddin, personal observation), suggesting that the dark colour is not derived from melanin, but from a yet unknown substance.

It is noteworthy that darkly coloured cornifications, similar to those of the claws of *X. laevis*, also occur in the claws of *O. japonicas* and the siren *P. striatus*, as well as in the keratinizing beaks of tadpoles in a wide variety of anuran species (e.g. *Rana*, *Hyla*, *Ceratophrys*, *Megophrys*; Kaung, 1975; Kaung & Kollros, 1977; Duellman & Trueb, 1994; Hosoi et al. 1996), and in the nuptial pads of many anurans [including *X. laevis* (Fig. 3A)] and caudates (e.g. *Notophthalmus viridescens*; Forbes et al. 1975). In agreement with a melanocyte-independent formation of these coloured structures, albino strains of *X. laevis* have been reported to have black claws and nuptial pads (Hoperskaya, 1975). The broad distribution of darkly coloured corneocytes among lissamphibians suggests that the process yielding the colour evolved in the common ancestor of frogs and salamanders and, as is known so far, that it is unique to lissamphibians. Thus, the occurrence of heavily cornified integument in some pedal digits of *X. laevis* may represent a localized activation of a process more generally widespread in lissamphibians.

Structural and developmental comparison of the claws of *Xenopus* and mammalian amniotes

Features of the microstructure of the cornified claw sheath in *X. laevis* that differ from those in the mouse can be attributed to differences in the pattern of cornified claw sheath development between the two taxa. Development of the claw in mammals begins in embryonic life (e.g. embryonic day 18 in rat; Hamrick, 2001, 2003; cat crown-rump length 13.5 mm; Kato, 1977) with the formation of the primary claw field or placode, which is identified as an epithelial thickening on the dorsodistal surface of the claw-bearing digit (Kato, 1977; Hamrick, 2001). This is followed by the formation of the proximal groove, which is then deepened into a fold by the rapidly proliferating germinative matrix cells located on the proximodorsal surface of the presumptive claw. Maddin et al. (2007) hypothesized that there was no such localized region

containing germinative matrix cells in *X. laevis*. This hypothesis is strongly supported by the developmental series and the results from PCNA staining presented here. The current morphological analyses show that at no point in development, or in adult animals, is there formation of a proximal groove containing any associated germinative matrix cells to form the cornified claw sheath in *X. laevis*. Instead, cells of the replacement layer along the entire length of the claw are incorporated into the cornified claw sheath.

In the mammalian claw, germinative matrix cells undergo terminal differentiation into corneocytes, which are then displaced distally over the epidermal claw bed to contribute to the cornified claw sheath (Kato, 1977; Hamrick, 2001, 2003; Homberger et al. 2009, this issue). Thus, the overall development of the mammalian claw sheath takes place in a proximal to distal direction. This is in contrast to the pattern of development of the cornified claw sheath in *X. laevis.* During development, layers of claw corneocytes accumulate from the differentiation process taking place along the entire length of the claw sheath, while the new layers are generated in the basal layer of the epidermis, generating a vertical growth pattern instead of a proximal to distal growth pattern. The growth in length of the claw of *X. laevis* is the result of a proximal extension of the cell layers that differentiate into modified claw sheath corneocytes rather than the result of displacement of claw sheath corneocytes distally towards the tip of the digit, as is the case in mammals.

In mammals, the rate of proliferation in different parts of the germinative matrix, as well as the firm attachment of the cornified claw sheath to the claw bed in the epidermis, along with the shape of the terminal phalanx, results in the particular morphology of the fully developed claw (Homberger et al. 2009, this issue). The gross morphology of the claw may vary among digits and between fore- and hindlimbs (Bryant et al. 1996); however, in general, the claw sheath is thinnest proximally and gradually thickens over the length of the germinative matrix. Furthermore, factors of geometry and proliferation kinetics also result in a distinctive shift in the orientation of the long axis of the corneocytes relative to the surface of the digit. Near the base of the cornified claw sheath the corneocytes are oriented obliquely to the surface of the digit. Distally, the angle between the long axis of the corneocytes and the surface decreases until they are almost parallel to each other, and to the surface of the digit, at the distalmosttip of the digit. In *X. laevis*, proliferation of living epidermal cells was detected in all regions underneath the cornified claw sheath, arguing against a separation into a germinative matrix and a putative equivalent of a distal nail or claw bed that does not contribute to the claw sheath accumulation found in the murine and human nail unit. Interestingly, the addition of corneocyte layers to the cornified claw sheath of *X. laevis* does not appear to be strictly synchronous with the formation of the cornified layer of the unmodified epidermis during the moulting cycle, as indicated by differences in the frequency of TUNEL-positive nuclei in the replacement layers underneath the cornified claw sheath and the adjacent unmodified epidermis. However, the conversion of living epidermal cells into corneocytes of the claw sheath appears to occur almost synchronously within the modified claw-forming epidermis.

The mechanism used by corneocytes in the cornified claw sheath to adhere to one another is another difference between the structure of the modified epidermis of the cornified claw sheaths of *X. laevis* and those of mammals. In *X. laevis*, large desmosomes that appear to be complete are located along the strongly interdigitated lateral margins of the claw sheath corneocytes. This type of zig-zag pattern present in the lateral cell walls occurs among the cells of the replacement layer underneath the cornified claw sheath as well as in the unmodified epidermis. Some interdigitations also occur on the apical and basal surfaces on the corneocytes of the cornified claw sheath in *X. laevis*; however, they are much less abundant than on the lateral surfaces. In this respect, the corneocytes of the claw sheath of *X. laevis* do not appear to differ greatly from those of the unmodified epidermis seen elsewhere on the body. Mammalian nail and claw corneocytes similarly utilize interdigitations to anchor the corneocytes to each other, but in contrast to the condition seen in *X. laevis*, the interdigitations are much finer and are not limited to the lateral margins, but occur in similar numbers on the apical and basal surfaces (Dawber et al. 1994).

In the absence of extensively interdigitating apical and basal margins, the mechanism for anchoring successive sheath layers is still unknown. Whereas desmosomes at the interface of the replacement layer and the cornified layer of the unmodified lissamphibian epidermis are broken during the shedding phase (Fox, 1986), it is conceivable that the desmosomes at this interface retain their ability to anchor cells to each other. A grainy matrix material was observed in the thin extracellular spaces between corneocyte layers in the cornified claw sheath of *X. laevis*. However, biochemical investigations are required to identify the matrix material and determine whether it possesses adhesive properties.

In summary, the structure and development of the claws of *X. laevis* show several apparently distinct features that are absent from claws of well-characterized amniote species such as the mouse. Accordingly, our data do not provide new support for a homologous relationship between claws of *X. laevis* and mammals. The similarity of the digital end organs of tetrapods appears to be restricted to commonalities in the hard physical properties, the anatomical localization and their epidermal origin. Recent comparative genetics studies have suggested that the main proteinaceous components of amniote claws, i.e.

hard alpha-keratins (Eckhart et al. 2008), keratin-associated proteins (Wu et al. 2008) and beta-keratins (Alibardi et al. 2007), originated after the divergence of the lissamphibian and amniote lineages. Convincing evidence for a putative origin of claws in a common ancestor of extant tetrapods remains to be found.

Acknowledgements

We would like to thank Drs M. Vickaryous and J.-Y. Sire for the opportunity to contribute to this special issue. We are grateful for the generous donations of material for this study from the Vize and MacFarlane Labs (University of Calgary), and J. P. Sundberg (The Jackson Laboratory, Bar Harbor, Maine). We are indebted to M. Vickaryous and W. Dong for their tremendous technical support, and the Anderson Lab (University of Calgary) for assistance with animal care. We would also like to thank H. Fischer, C. Barresi, E. Tschachler and L. Alibardi for numerous fruitful discussions, and the comments from the reviewers for improving the quality of the manuscript. Funding for this study was provided by NSERC (HCM, APR) and Alberta Ingenuity (HCM).

References

Alibardi L (2001) Keratinization in the epidermis of amphibians and the lungfish: comparison with amniote keratinization. *Tissue Cell* **33**, 439–449.

Alibardi L (2003) Ultrastructural localization of histidine-labelled interkeratin matrix during keratinization of amphibian epidermis. *Acta Histochemica* **105**, 273–283.

Alibardi L (2008) Microscopic analysis of lizard claw morphogenesis and hypothesis on its evolution. *Acta Zool (Stockholm)* **89**, 169–178.

Alibardi L, Toni M (2004) Immuno-cross reactivity of Transglutaminase and cornification marker proteins in the epidermis of vertebrates suggests common processes of soft cornification across species. *J Exp Zool (Mol Dev Evol)* **302B**, 526–549.

Alibardi L, Toni M, Valle LD (2007) Hard cornification in reptilian epidermis in comparison to cornification in mammalian epidermis. *Exp Dermatol* **16**, 961–976.

Bani G (1966) Osservazioni sulla ultrastructtura della cute di *Bufo bufo* (L.) e modificazioni a livello dell'epidermide, in relazione a differenti condizioni ambientali. *Monit Zool Ital* **74**, 93–124.

Bragulla H, Ernsberger S, Budras K-D (2001) On the development of the papillary body of the feline claw. *Acta Histol Embryol* **30**, 211–217.

Bryant HN, Russell AP, Laroiya R, Powell GL (1996) Claw retraction and protraction in the Carnivora: skeletal microvariation in the phalanges of the Felidae. *J Morphol* **229**, 289–308.

Budtz PE, Larsen LO (1973) Structure of the toad epidermis during the moulting cycle. I. Light microscopic observations in *Bufo bufo* (L.). *Z Zellforsch Mikrosk Anat* **144**, 353–368.

Budtz PE, Larsen LO (1975) Structure of toad epidermis during the moulting cycle. II. Electron microscopic observations in *Bufo bufo* (L.). *Cell Tissue Res* **159**, 459–483.

Dawber RPR, de Berker D, RB (1994) Science of the nail apparatus. In *Diseases of the Nails and Their Management* (eds Baran R, Dawber RPR, Berker D de, Haneke E, Tosti A), pp. 1–34. Oxford: Blackwell Science.

de Berker D, Angus B (1996) Proliferative compartments in the normal nail unit. *Br J Dermatol* **135**, 555–559.

Duellman WE, Trueb L (1994) *Biology of Amphibians*. Baltimore: The Johns Hopkins University Press.

Eckhart L, Valle LD, Jaeger K, et al. (2008) Identification of reptilian genes encoding hair keratin-like proteins suggests a new scenario for the evolutionary origin of hair. *Proc Natl Acad Sci U S A* **105**, 18419–18423.

Estabel J, Mercer A, König N, Exbrayat JM (2003) Programmed cell death in *Xenopus laevis* spinal cord, tail and other tissues, prior to, and during, metamorphosis. *Life Sci* **73**, 3297–3306.

Fischer H, Eckhart L, Mildner M, et al. (2007) DNase1L2 degrades nuclear DNA during corneocyte formation. *J Invest Dermatol* **127**, 24–30.

Forbes MS, Dent JN, Singhas CA (1975) The developmental cytology of the nuptial pad in the red-spotted newt. *Dev Biol* **46**, 56–78.

Fox H (1986) The skin of amphibia. Epidermis. In: *Biology of the Integument. Vol. 2, Vertebrates* (eds Bereiter-Hahn J, Matoltsy AG, Richards KS), pp. 78–110. New York: Springer.

Frost DR, Grant T, Faivovich J, et al. (2006) The amphibian tree of life. *Bull Am Mus Nat History* **297**, 1–370.

Hamrick MW (2001) Development and evolution of the mammalian limb: adaptive diversification of nail, hooves, and claws. *Evol Devel* **3**, 355–363.

Hamrick MW (2003) Evolution and development of mammalian limb integumentary structures. *J Exp Zool (Mol Dev Evol)* **298B**, 152–163.

Homberger DG, Ham K, Ogunbakin T, et al. (2009) The structure of the cornified claw sheath in the domesticated cat (*Felis catus*): implications for the claw-shedding mechanism and the evolution of cornified digital end organs. *J Anat* **214**, 620–643.

Hoperskaya OA (1975) The development of animals homozygous for a mutation causing periodic albinism (ap) in *Xenopus laevis*. *J Embryol Exp Morphol* **34**, 253–264.

Hosoi M, Hasegawa Y, Ueda H, Maeda N (1996) Scanning electron microscopy of the mouthparts in the anuran tadpole Rhacophoridae, *Buergeria buergeri*. *J Electron Microsc* **45**, 477–482.

Jaeger K, Fischer H, Tschachler E, Eckhart L (2007) Terminal differentiation of nail matrix keratinocytes involves up-regulation of DNase1L2 but is independent of caspase-14 expression. *Differentiation* **75**, 939–946.

Jorgensen CB, Larsen LO (1964) Further observations on molting and its hormonal control in *Bufo bufo* (L.). *Gen Comp Endocrinol* **4**, 389–400.

Kato T (1977) A study on the development of the cat claw. *Hiroshima J Med Sci* **26**, 103–126.

Kaung H-LC (1975) Development of the beaks of *Rana pipiens* larvae. *Anat Rec* **182**, 401–414.

Kaung H-LC, Kollros JJ (1977) Cell turnover in the beak of *Rana pipiens*. *Anat Rec* **188**, 361–370.

Lavker RM (1974) Horny cell formation in the epidermis of *Rana pipiens*. *J Morph* **142**, 365–378.

Maddin HC, Musat-Marcu S, Reisz RR (2007) Histological microstructure of the claws of the African clawed frog, *Xenopus laevis* (Anura: Pipidae): implications for the evolution of claws in tetrapods. *J Exp Zool (Mol Dev Evol)* **308B**, 259–268.

Nieuwkoop PD, Faber J (1967) Normal table of *Xenopus laevis* (Daudin). Amsterdam: North-Holland Publishing.

Noble GK (1931) *The Biology of the Amphibia*. New York: Dover Publications, Inc.

Parakkal PF, Matoltsy AG (1964) A study of the fine structure of the epidermis of *Rana pipiens*. *J Cell Biol* **20**, 85–94.

Plikus M, Wang WP, Liu J, Wang X, Jiang TX, Chuong CM (2004) Morphoregulation of ectodermal organs: integument pathology

and phenotypic variation in K14-Noggin engineered mice through modulation of bone morphogenic protein pathway. *Am J Pathol* **164**, 1099–1114.

San Mauro D, Vences M, Alcobendas M, Zardoya R, Meyer A (2005) Initial diversification of living amphibians predated the breakup of Pangaea. *Am Nat* **165**, 590–599.

Witten PE, Hall BK (2003) Seasonal changes in the lower jaw skeleton in male Atlantic salmon (Salmo salar L.): remodeling and regression of the kype after spawning. *J Anat* **203**, 435–450.

Wu DD, Irwin DM, Zhang YP (2008) Molecular evolution of the keratin associated protein gene family in mammals, role in the evolution of mammalian hair. *BMC Evol Biol* **8**, 241.